Zheng et al. Satellite Navigation (2022) 3:9
https://doi.org/10.1186/s43020-022-00070-6

Satellite Navigation
https://satellite-navigation.springeropen.com/

ORIGINAL ARTICLE

Open Access

Satellite integrity monitoring for satellite-based augmentation system: an improved covariance-based method

Shuaiyong Zheng[1*], Mengzhi Gao[1], Zhigang Huang[2], Xiaoqin Jin[3] and Kun Li[1]

Abstract

Satellite integrity monitoring is vital to satellite-based augmentation systems, and can provide the confidence of the differential corrections for each monitored satellite satisfying the stringent safety-of-life requirements. Satellite integrity information includes the user differential range error and the clock-ephemeris covariance which are used to deduce integrity probability. However, the existing direct statistic methods suffer from a low integrity bounding percentage. To address this problem, we develop an improved covariance-based method to determine satellite integrity information and evaluate its performance in the range domain and position domain. Compared with the direct statistic method, the integrity bounding percentage is improved by 24.91% and the availability by 5.63%. Compared with the covariance-based method, the convergence rate for the user differential range error is improved by 8.04%. The proposed method is useful for the satellite integrity monitoring of a satellite-based augmentation system.

Keywords: Clock-ephemeris covariance matrix, Groove model, Satellite-based augmentation system, Scale model, User differential range error

Introduction

Satellite-Based Augmentation System (SBAS) provides the differential corrections and integrity information to Global Navigation Satellite System (GNSS) users or SBAS users, enhancing the accuracy and integrity of GNSS services. With the signals of SBAS satellites used for ranging, SBAS also enhances the continuity and availability of GNSS (Meng & Hsu, 2021; SC-159, 2016), as shown in Fig. 1.

To guarantee flight safety, the integrity information of GNSS navigation signals shall be determined for aviation users. The integrity information includes the User Differential Range Error (UDRE) and the clock-ephemeris covariance matrix. Their stringent safety-of-life requirements are described in the document (SC-159, 2016). Specifically, the integrity information denotes the uncertainty of satellite corrections. It sets the tolerances of the SBAS correction errors, further the user's Horizontal Protection Level (HPL) and Vertical Protection Level (VPL) (Lu et al., 2021).

How to determine the satellite integrity information satisfying the requirement of flight safety is always a topic of SBAS. The existing satellite integrity algorithms are mainly divided into the Covariance-Based (CB) methods and the Direct Statistic (DS) methods.

The covariance-based methods have attracted a great attention for many years. Tsai (1999) adopted the weighted least squares to estimate the UDRE with the covariance matrix for the combined ephemeris and clock errors. But Shao (2012) demonstrated that sometimes the UDRE deduced with the Tsai's method cannot bound the residual errors. Walter, et al. (2001) first put forward a new message named Message Type 28 (MT28) which contains a relative clock and ephemeris covariance

*Correspondence: 18810761681@139.com

[1] School of Integrated Circuit Science and Engineering, Tianjin University of Technology, No. 391 Bin Shui Xi Dao Road, Xiqing District, Tianjin 300384, China
Full list of author information is available at the end of the article

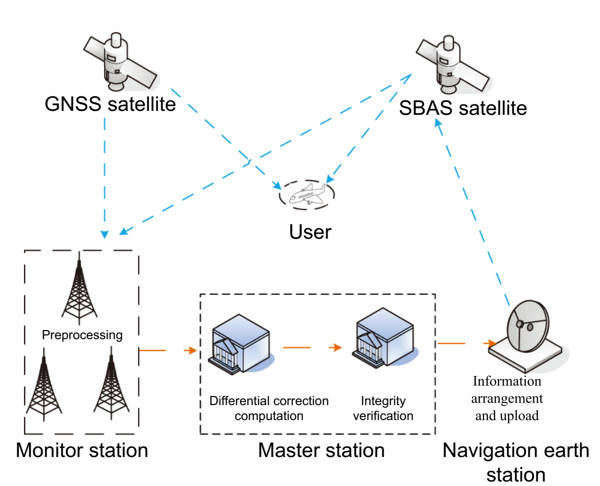

Fig. 1 Satellite integrity monitoring system for SBAS (Li et al., 2020)

matrix for individual satellites. The covariance matrix is a location-specific modifier used to adjust the broadcast UDRE values as a function of the user's position (SC-159, 2016). From this matrix users can reconstruct their location-specific error bound rather than applying the largest bound in the service volume, improving the availability within the service volume and the integrity outside the service volume (Walter et al., 2001). Wu and Peck (2002) proposed two methods with the consideration of false alert rate and missed detection probability to construct shape covariance and used them to find the best covariance with the prototype software of the Wide Area Augmentation System (WAAS). The computational time of the proposed method is longer than that provided by the method at the time. Blanch et al. (2012) proposed a complex algorithm to compute the error bounds of the clock and ephemeris for dual frequency SBAS with service volume analysis tool MAAST (MATLAB Algorithm Availability Simulation Tool). Shao et al. (2011a) analyzed the projection of the clock-ephemeris covariance in the direction of pseudorange, and developed an analytical method to solve for UDRE by simulation data, but did not provide the service performance (Shao, 2012). Chen et al. (2018) put forward a pseudorange residuals-based method to compute the clock-ephemeris covariance for dual-frequency multi-constellation SBAS, neglecting the effects of fat tails.

The direct statistic methods are discussed several times. Chen (2001) gave the formula to compute UDRE and showed the initial results. Also, Li (2018) gathered the statistics of range errors from clock-ephemeris to determine UDRE which can only bound the range errors from clock-ephemeris at the probability of 75%, not satisfying the integrity requirement (Li et al., 2018, 2019). Obviously, the direct statistic method is not a proper method to create an integrity bound as it will never accumulate enough independent samples in any feasible time frame. The residual errors shall be overbounded using the threat models that consider other information about the possible magnitude of the error.

Moreover, BeiDou-3 navigation satellite System (BDS-3) was completed a few years ago, and Global Positioning System (GPS) has been fully operational since 1995. BeiDou Satellite-Based Augmentation System (BDSBAS) was just constructed, while WAAS passed test certification and started providing services to civil users in 2003. Thus, BDSBAS urgently needs a satellite integrity monitoring method under the conditions that its monitor stations are deployed in the domestic region and their layout is limited. BDSBAS faces many difficulties in integrity monitoring, especially in the south of the inverted triangle and the edge area of the monitoring network.

Although several algorithms have been developed for satellite integrity monitoring, there are some problems to be solved. Since SBAS has a top-level safety requirement, any integrity risk issues shall be considered. The direct statistic methods cannot provide UDRE and MT28 accurately, and the integrity bounding rate in the range domain is too low to bound the range error from the clock-ephemeris. The latest CB method noted as the WAAS CB method shows a good performance with the dependence on three expensive receivers set at a monitor station and overseas monitoring network layout, which is not applicable to Chinese BDSBAS. The problems are how to estimate integrity information accurately and improve the integrity bounding rate in the range domain and develop a method suitable for Chinese monitoring network layout or terrain, which motivates the authors to put forward a method for satellite integrity monitoring.

An improved covariance-based method is developed to determine satellite integrity information. Firstly, the covariance matrix of satellite clock-ephemeris correction errors output from the correction processor is adjusted by a scale model and a groove model. Subsequently, the adjusted matrix is decomposed into the user differential range errors and clock-ephemeris covariance matrix. Finally, the performance of the proposed method is analyzed in the range domain and position domain. Compared with the direct statistic method, the integrity bounding rate and the availability are both improved obviously. Compared with the covariance-based method, the convergence rate for the user differential range error is faster by 8.04%. The contributions are listed as follows:

1. An improved covariance-based method is proposed to perform satellite integrity monitoring. The user equivalent range error is used to adjust the shape of

the covariance of clock-ephemeris reducing the computational complexity, and the geometry between satellites and monitor stations is taken as new information source to compensate for the insufficient monitoring capability of monitor stations when a monitored satellite is moving over the boundary of the monitoring network. The geometry of the satellite and monitor stations is used to mitigate the random error or integrity threats improving the accuracy of the estimated satellite integrity information.

2. A groove model is developed to adjust the clock-ephemeris covariance and find a suitable shape covariance matrix. This model is used to construct a near- optimal solution rather than the theoretically best broadcast covariance matrix, which needs complicated computation. When a satellite is under a bad monitoring geometry, both the pseudorange residuals and the geometry information are used to determine the modifier for the clock-ephemeris covariance. The model provides an idea to perform satellite integrity monitoring by considering the motion process of a satellite above its monitoring network.

This article is arranged as the following. Section II describes the preliminaries of satellite integrity and the problem under discussion. Section III presents the model and the process to deduce satellite integrity information. In Section IV, the performance of the proposed method is compared with the state-of-the-art methods. Section V concludes the advantages and characteristics of the proposed method.

Preliminaries and problem formulation

In this section, the concept of UDRE and its modifier (or MT28) is introduced in the subsection preliminaries, which is the basis of satellite integrity monitoring. Then, the problem under consideration and the research objective are given in the subsection problem formulation.

Preliminaries

Satellite corrections include long-term corrections and fast corrections which are used to revise the slowly changing errors and rapidly changing errors of Satellite Clock-Ephemeris (SCE), respectively. The accuracy of the combined long-term and fast corrections is indicated by UDRE along with MT28.

The definition of UDRE was put forward in the early version of RTCA DO-229 (SC-159, 2016). The UDRE is used as the confidence limit of pseudorange residual errors corresponding to the satellite corrections at any point of the service volume of a monitored satellite in space and time. The UDRE is broadcast to support HPL and VPL by bounding the Horizontal Position Error (HPE) and Vertical Position Error (VPE) with a required probability, respectively. The UDRE is quantified by UDRE Index (UDREI) and the UDRE value represented by each indexed value is listed in the lookup table (SC-159, 2016). The table gives both a 3.29 sigma value (UDRE) and a 1 sigma value σ_{UDRE} relative to clock-ephemeris errors (Wu & Peck, 2002).

Afterwards, the MT28 was proposed to improve the integrity and availability of SBAS. The MT28 provides the 10 entries of an upper triangular matrix which is used to construct a relative clock-ephemeris covariance matrix and further a location-specific error bound for each monitored satellite (Walter et al., 2001). Then, the satellite correction errors are bounded by UDRE along with the associated MT28. The UDRE along with MT28 represents the clock-ephemeris error bound and a user-level error limit in the line of sight between each satellite-user pair.

Problem formulation

In this subsection, the authors will present a detailed description of the problem under consideration.

In the direct statistic method, the integrity parameter σ^2_{UDRE,DS^i} is given by (Li, 2018)

$$\sigma^2_{UDRE,DS^i} = \left(\left| d\overline{\rho}^i \right| + \sqrt{\frac{1}{N-1} \sum_j \sum_k \left(d\rho^i_{j,k} - d\overline{\rho}^i \right)^2} \right)^2 \tag{1}$$

where the designators i, j and k represent the satellite, monitor station, and epoch, respectively. $\mathrm{d}\rho^i_{j,k}$ denotes the pseudorange residual between satellite i and station j. The variable $\mathrm{d}\overline{\rho}^i$ denotes the mean of the set $\left\{\mathrm{d}\rho^i_{j,k}\right\}$ during a UDRE update period. Then, UDRE is obtained according to the lookup table (SC-159, 2016).

This method demonstrates that the computed UDRE only bounds the pseudorange residual $\mathrm{d}\rho^i_{j,k}$ with the probability of 75% approximately (Li, 2018; Li et al., 2018, 2019). Obviously, there are some shortcomings of the direct statistic method. Basically, the integrity bounding rate shall be calculated by UDRE along with MT28, not only UDRE. Conclusively, the UDRE cannot bound the clock-ephemeris range residuals for individual satellites with a prescribed probability, and the integrity bounding rate is too low to meet the confidence level of satellite corrections.

Essentially, since the samples of the set $\left\{\mathrm{d}\rho^i_{j,k}\right\}$ are never adequate, UDRE cannot be precisely obtained (Decleene, 2000). The direct statistic method is not a proper method to create an integrity bound as it will never accumulate enough independent samples in any feasible time frame. The residual errors shall be overbounded using the threat models that consider other information about the possible magnitude of the error.

As for the WAAS CB method, its characteristics can be listed as follows:

1. The WAAS CB method strongly depends on the performance of three sets of monitor station receivers which are costly. With three sets of receivers, WAAS shows a good performance, but the construction cost of monitor stations is quite high. The cost of each WAAS monitor station is millions of dollars, dozens of times that of each Chinese monitor station.
2. The WAAS CB method is closely related to the layout of monitor stations, and the performance of WAAS in the continental United States is ensured only by the broad layout of WAAS monitor stations some of which are deployed in Central Pacific, Canada, and Mexico. The WAAS CB method do not discuss how to perform satellite integrity monitoring under a limited monitoring network layout (or terrain) or in the edge area of the monitoring network.
3. WAAS is developed for civil applications, and the latest satellite integrity algorithm for WAAS aims at the improvement of integrity for safety-of-life users. WAAS algorithm emphasizes the integrity in range domain and position domain (Chen et al., 2018). To ensure the integrity of WAAS, the accuracy of Signal-In-Space (SIS) of WAAS is conservative and is not enough for precise positioning application (Chen et al., 2017b; Zheng et al., 2019, 2022).

In a word, satellite integrity monitoring for satellite-based augmentation system in China faces many difficulties. DS method shows a low integrity bounding rate, and the current domestic satellite integrity monitoring cannot satisfy the requirements of SBAS. The latest covariance-based method noted as the WAAS CB method relies on high quality monitor stations and their broad layout, which is different from Chinese situations. However, the WAAS CB method sacrifices SIS accuracy for satellite integrity.

The problem under consideration is how to determine the confidence limit for satellite corrections. Specifically, the problem under discussion is how to perform satellite integrity monitoring under the monitor stations with limited quality and their limited layout. Three assumptions are given below: 1) The pseudorange between a satellite-monitor station pair contains satellite clock-ephemeris errors, and can be used to monitor the status of each satellite; 2) User equivalent range errors between satellites and monitor stations reflect the monitoring capability of a monitoring network composed of widely distributed monitor stations, and can be used to determine a suitable shape covariance matrix for satellite clock-ephemeris; 3) The geometry between satellites and monitor stations is relative to the monitoring capability of the monitoring network, and can be used to find the suitable shape covariance matrix of satellite clock-ephemeris. The objective is to develop a method to determine UDRE and MT28 for each monitored satellite.

Determination of integrity information for SBAS

In this section, a scale model and a groove model are developed for SBAS to perform satellite integrity monitoring.

Scale model based on multiple error sources

The pseudorange correction error $\mathrm{d}\rho$, namely User Equivalent Range Error (UERE), for a specific satellite is computed by

$$\mathrm{d}\rho = \Delta\rho - \Delta\boldsymbol{R} \cdot \boldsymbol{I} + \Delta B \tag{2}$$

where the variables $\Delta\rho, \Delta\boldsymbol{R}, \Delta B$ represent the synchronized pseudorange residual from monitor stations, the total long-term corrections computed by long-term satellite error corrections, and the total fast corrections computed by fast corrections and range-rate corrections, respectively. The 4×1 vector $\boldsymbol{I}$ consists of a unit vector and one element -1. The first three terms of this vector are the components of the unit vector along the line of sight in Earth-Centered Earth-Fixed (ECEF) coordinates (Wu & Peck, 2002).

Specifically, the pseudorange residual in (2) due to the ephemeris and clock for a satellite-user pair with the line of sight $\boldsymbol{I}$ is theoretically given by (Blanch et al., 2012)

$$\mathrm{d}\rho_{\mathrm{SCE}} = \boldsymbol{I}^{\mathrm{T}}(\boldsymbol{x}_{\mathrm{BD}} - \boldsymbol{x}) \tag{3}$$

where $\boldsymbol{x}$ and $\boldsymbol{x}_{\mathrm{BD}}$ represent the true clock-ephemeris, and the clock-ephemeris computed by broadcast ephemeris and SBAS corrections, respectively. UDRE along with MT28 is the upper bound on this pseudorange residual for each satellite-user pair. According to SC-159 (2016), the error bound is expressed in the following form (Blanch et al., 2014)

$$L = K_7\sigma_{\mathrm{flt}} = K_7\sigma_{\mathrm{UDRE}}\sqrt{\boldsymbol{I}^{\mathrm{T}}\boldsymbol{C}_{\mathrm{MT28}}^{\mathrm{ov}}\boldsymbol{I}} \tag{4}$$

where the matrix $\boldsymbol{C}_{\mathrm{MT28}}^{\mathrm{ov}}$ is a 4 by 4 matrix. The parameter K_7 denotes the quantile of 99.99999%. The parameter σ_{flt} denotes the clock-ephemeris standard deviation determined by UDRE and MT28.

To deduce the error bound for clock-ephemeris, there are four cases to be considered (Blanch et al., 2012): (1) nominal errors from the monitoring network receivers;

(2) nominal biases or antenna biases; (3) satellite correction errors; (4) possibly undetected errors in the monitoring network receivers where one station is assumed to return erroneous measurements.

As for case (1), the relationship between the bound on the estimation error and the probability P_{HMI} of Hazardously Misleading Information (HMI) is described by

$$P\left(\left|\boldsymbol{I}^{\mathrm{T}}(\hat{\boldsymbol{x}}-\boldsymbol{x})\right| \geq K_{\mathrm{HMI}}\sqrt{\boldsymbol{I}^{\mathrm{T}}\boldsymbol{P}_{\mathrm{SCE}}\boldsymbol{I}}\right) = P_{\mathrm{HMI}} \tag{5}$$

where K_{HMI} represents the quantile related to the probability P_{HMI} and $\boldsymbol{P}_{\mathrm{SCE}}$ denotes the covariance for the state $\hat{\boldsymbol{x}}$ of clock-ephemeris. The probability P_{HMI} is determined by an integrity allocation strategy (Lu et al., 2021; SC-167, 1992; Schempp et al., 2001; Wu & Peck, 2002).

According to (5), the error bound on the estimation error under the nominal conditions is given by

$$L_1 = K_{\mathrm{HMI}}\sqrt{\boldsymbol{I}^{\mathrm{T}}\boldsymbol{P}_{\mathrm{SCE}}\boldsymbol{I}} \tag{6}$$

The bound L_1 is one upper bound on clock-ephemeris errors before the clock-ephemeris covariance matrix is broadcast. The nominal biases $\boldsymbol{b}$ such as antenna biases and Code Noise and Multi-Path (CNMP) termed as the case (2) is described as a Gaussian vector with expectation $\overline{\boldsymbol{b}}$ and covariance $\boldsymbol{W}^{-1}$. As for the line of sight, the contribution of these biases can be given by $\boldsymbol{I}^{\mathrm{T}}\boldsymbol{H}\boldsymbol{b}$. An upper bound of this variable is deduced by (Blanch et al., 2012)

$$K_{\mathrm{bias}} = \max_{\boldsymbol{b}} \sqrt{\boldsymbol{b}^{T}\boldsymbol{W}\boldsymbol{b}} = \sqrt{\boldsymbol{b}_{\max}^{\mathrm{T}}\boldsymbol{W}\boldsymbol{b}_{\max}} \tag{7}$$

The parameter K_{bias} associated with antenna biases is calculated in real time as a function of its covariance and the maximum biases (Shallberg & Sheng, 2008). Therefore, when case (2) is considered, the error bound on the estimation error is adjusted by

$$L_2 = (K_{\mathrm{HMI}} + K_{\mathrm{bias}})\sqrt{\boldsymbol{I}^{\mathrm{T}}\boldsymbol{P}_{\mathrm{SCE}}\boldsymbol{I}} \tag{8}$$

where L_2 denotes the bound for clock-ephemeris errors under cases (1) and (2).

When the error from the broadcast clock-ephemeris or the quantization error of satellite corrections termed as the case (3) is considered, the upper bound for this error can be deduced by the following inequality

$$\begin{aligned}\left|I^{T}(x_{BD}-\hat{x})\right| &= \left|I^{T}P_{SCE}^{0.5}P_{SCE}^{-0.5}(x_{BD}-\hat{x})\right| \\ &\leq \sqrt{(x_{BD}-\hat{x})^{T}P_{SCE}^{-1}(x_{BD}-\hat{x})}\sqrt{I^{T}P_{SCE}I}\end{aligned} \tag{9}$$

Let

$$K_{\mathrm{pfa}} = \max_{i}\sqrt{\left(\boldsymbol{x}_{\mathrm{BD},i}-\hat{\boldsymbol{x}}_i\right)^{\mathrm{T}}\boldsymbol{P}_{\mathrm{SCE}}^{-1}\left(\boldsymbol{x}_{\mathrm{BD},i}-\hat{\boldsymbol{x}}_i\right)} \tag{10}$$

The designator i represents the epoch of each update interval. When case (3) is taken into consideration, the error bound on the estimation error is updated by

$$L_3 = \left(K_{\mathrm{HMI}} + K_{\mathrm{bias}} + K_{\mathrm{pfa}}\right)\sqrt{\boldsymbol{I}^{\mathrm{T}}\boldsymbol{P}_{\mathrm{SCE}}\boldsymbol{I}} \tag{11}$$

Obviously, the new error bound satisfies

$$P\left(\left|\boldsymbol{I}^{\mathrm{T}}(\hat{\boldsymbol{x}}-\boldsymbol{x})\right| \geq \left(K_{\mathrm{HMI}} + K_{\mathrm{bias}} + K_{\mathrm{pfa}}\right)\sqrt{\boldsymbol{I}^{\mathrm{T}}\boldsymbol{P}_{\mathrm{SCE}}\boldsymbol{I}}\right) \leq P_{\mathrm{HMI}} \tag{12}$$

which is in accordance with the constraint (5).

As for case (4), the reliability of each monitor station can be guaranteed by checking the observations of multiset receivers which refers to a problem of data quality monitoring or system reliability (Hamada, 2008; Yin & Chai, 2020). As for WAAS monitor stations, three sets of receivers are equipped to collect observations (Parkinson et al., 1996). The observations from three receivers are used to conduct the cross check among three threads to remove erroneous observations (Parkinson et al., 1996; Shallberg & Sheng, 2008). Moreover, dual frequency pseudoranges can be smoothed by dual frequency carriers, and the related algorithm like IFree filter is chosen to improve the quality of the observations simultaneously with ionospheric delay removed (Hwang et al., 1999; Konno et al., 2006).

Before message type 28 is broadcast, the covariance matrix of clock-ephemeris needs to be adjusted to meet the integrity requirement. According to (4) and (11), the adjusted covariance matrix can be obtained by

$$\boldsymbol{P}_1 = \left(\frac{L_3}{L}\right)^2\boldsymbol{P}_{\mathrm{SCE}} = \left(\frac{K_{\mathrm{HMI}} + K_{\mathrm{bias}} + K_{\mathrm{pfa}}}{K_7}\right)^2\boldsymbol{P}_{\mathrm{SCE}} \tag{13}$$

The matrix denotes the clock-ephemeris covariance considering four cases.

After the message type 28 is available, the quantization error related to this message type needs to be protected either by the term ε_C or by increasing the broadcast UDRE (Walter et al., 2001). Computing the theoretically optimal matrix $\boldsymbol{P}_{\mathrm{brdc}}$ refers to a complicated mathematical problem, and a near-optimal method is adopted in practice. The authors choose a scaling method where the matrix $\boldsymbol{P}_{\mathrm{brdc}}$ is obtained by finding a suitable shape covariance matrix and then scaling it so that the integrity safety condition is met (Walter et al., 2001; Wu & Peck, 2002). The integrity condition to be satisfied is

$$\sigma_{\mathrm{UDRE}}\delta_{\mathrm{UDRE}} \geq \sqrt{\boldsymbol{I}^{\mathrm{T}}\boldsymbol{P}_1\boldsymbol{I}} \tag{14}$$

$$\frac{\sigma_{\mathrm{UDRE}}}{\sqrt{P_{\max}}} \geq \frac{\sqrt{\boldsymbol{I}^{\mathrm{T}}\boldsymbol{P}_1\boldsymbol{I}}}{\delta_{\mathrm{UDRE}}\sqrt{P_{\max}}} = \frac{\sqrt{\boldsymbol{I}^{\mathrm{T}}\boldsymbol{C}\boldsymbol{I}}}{\delta_{\mathrm{UDRE}}} = \frac{\sqrt{\boldsymbol{I}^{\mathrm{T}}\boldsymbol{C}\boldsymbol{I}}}{\sqrt{\boldsymbol{I}^{\mathrm{T}}\boldsymbol{C}_{\mathrm{brdc}}\boldsymbol{I}} + \varepsilon_C} \tag{15}$$

Then, the covariance matrix can be adjusted again by

$$\boldsymbol{P}_2 = \left(\frac{\sigma_{\mathrm{UDRE}}^2}{P_{\max}}\right)\left(\frac{K_{\mathrm{HMI}} + K_{\mathrm{bias}} + K_{\mathrm{pfa}}}{K_7}\right)^2 \boldsymbol{P}_{\mathrm{SCE}} \tag{16}$$

where the parameter $P_{\max}$ is deduced by

$$P_{\max} = \max_{\boldsymbol{I}\in\boldsymbol{I}_{\mathrm{sv}}}\left(\boldsymbol{I}^{\mathrm{T}}\boldsymbol{P}_{\mathrm{SCE}}\boldsymbol{I}\right) = \boldsymbol{I}_{\mathrm{WUL}}^{\mathrm{T}}\boldsymbol{P}_{\mathrm{SCE}}\boldsymbol{I}_{\mathrm{WUL}} \tag{17}$$

The set $\boldsymbol{I}_{\mathrm{SV}}$ represents all the 4 by 1 vectors located in the Service Volume (SV) of a monitored satellite. The Worst User Location (WUL) is determined by an analytic method (Shao et al., 2011a; Zhao et al., 2014).

In (16), the true value of σ_{UDRE} is not known and therefore an overbound must be determined. Under the assumption that the range error $\mathrm{d}\rho$ from the clock-ephemeris satisfies the condition $\mathrm{d}\rho \sim \mathrm{N}(\mu, \sigma^2)$, the following formula can be obtained

$$P\left(\left|\mathrm{d}\rho - \mu\right| \geq K_{\mathrm{HMI}}\sigma\right) \leq P_{\mathrm{HMI}} \tag{18}$$

Considering the inequality

$$P\left(\left|\mathrm{d}\rho - \mu\right| \geq K_{\mathrm{HMI}}\sigma\right) \geq P\left(\left|\mathrm{d}\rho\right| - |\mu| \geq K_{\mathrm{HMI}}\sigma\right) \tag{19}$$

the following inequality can be obtained

$$P\left(\left|\mathrm{d}\rho\right| \geq K_{\mathrm{HMI}}\left(\frac{|\mu|}{K_{\mathrm{HMI}}} + \sigma\right)\right) \leq P_{\mathrm{HMI}} \tag{20}$$

Hence, the Gaussian distribution $\mathrm{N}\left(\mu, \left(\frac{|\mu|}{K_{\mathrm{HMI}}} + \sigma\right)^2\right)$ is used to find the bound of $\mathrm{d}\rho$ and its standard deviation is computed by

$$s = \frac{\left|\mathrm{d}\overline{\rho}\right|}{K_{\mathrm{HMI}}} + \sigma(\mathrm{d}\rho) \tag{21}$$

Several situations are taken to tackle the integrity threats. Firstly, to meet the strict Gaussian overbounding properties required by the WAAS integrity monitoring, the CNMP algorithm including mean filter and mean error function is adopted to reduce the effects of multipath (Decleene, 2000; Shallberg et al., 2001). Secondly, the right tail Cumulative Distribution Function (CDF) is used to bound the probability of HMI, and the thresholds for the error in the corrections and the noise in the measurements can be derived (Schempp et al., 2001). More importantly, the authors also develop a model to improve the monitoring capability of monitor stations, which will be introduced below.

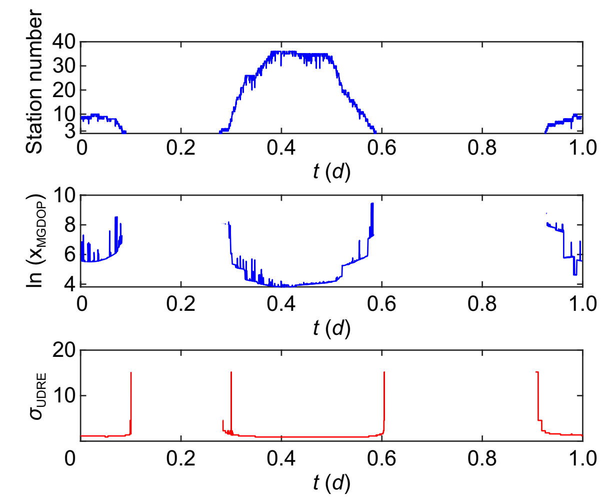

Fig. 2 Relationship between $\ln(x_{MGDOP})$ and WAAS-reported σ_{UDRE}

Groove model based on satellite-station geometry

In this subsection, a model is constructed to improve the performance of the bound of clock-ephemeris range errors. The algorithm for s is adjusted under different situations. A groove model is proposed to provide a solution.

To improve the insufficient monitoring capability of monitor stations when a satellite is moving over the boundary of the monitoring network, the geometry between the satellite and monitor stations is introduced as a kind of prior information to overcome the shortcomings of the method to determine the parameters.

The geometry of these monitor stations tracking a specific satellite is evaluated by Monitoring Geometric Dilution Of Precision (MGDOP), or further $\ln(x_{MGDOP})$ which is computed by the corresponding geometry matrix (Chen et al., 2017a). The relationship between MGDOP and UDREI is analyzed in (Chen et al., 2017a; Shao et al., 2009, 2011a). Based on this, the geometric information is used to adjust the shape of the clock-ephemeris covariance to ensure the satellite integrity. Taking satellite PRN 6 as an example, the number of the monitor stations tracking PRN6 and the WAAS-reported σ_{UDRE} of PRN6 for one day are shown in Fig. 2. The lateral axis denotes time (t) in unit of day (d).

As shown in Fig. 2, the number of the monitor stations varies from 0 to over 30 and changes fast. Accordingly, $\ln(x_{MGDOP})$ varies conversely and synchronously. The trend of σ_{UDRE} is the same as that of $\ln(x_{MGDOP})$, and $\ln(x_{MGDOP})$ can be taken as supplementary information to deduce s. Apparently, the trend of σ_{UDRE} or $\ln(x_{MGDOP})$ for all satellites likes a groove. Therefore, the geometry of a specific satellite and the monitor stations, namely, MGDOP, can be taken as the boundary condition and further used to compensate the algorithm for deducing s, denoted as s_{DOP}. Based on these, a groove model is developed to describe the trend of s as illustrated in Fig. 3.

According to this model, the algorithms to compute s are given by

$$s_1 = \begin{cases} \max\left(s, s_{\mathrm{limit}}\right), \mathrm{N}\left(U_{90,15}\right) \geq N_0 \\ \max\left(s, s_{\mathrm{limit}}, s_{\mathrm{DOP}}\right), \mathrm{N}\left(U_{90,15}\right) < N_0 \& \mathrm{N}\left(U_{90,5}\right) \geq 4 \\ \mathrm{NaN}, \text{otherwise} \end{cases} \tag{22}$$

where the parameters s and s_{DOP} are computed by user equivalent range errors and geometry information, respectively, and NaN denotes not a number. For simplicity, let $U_{\alpha_{\mathrm{EL}(2)},\alpha_{\mathrm{EL}(1)}}$ denote the set of UEREs with their ELevation angle (EL) α_{EL} under the condition $\alpha_{\mathrm{EL}(1)} \leq \alpha_{\mathrm{EL}} \leq \alpha_{\mathrm{EL}(2)}$ and $\mathrm{N}\left(U_{\alpha_{\mathrm{EL}(2)},\alpha_{\mathrm{EL}(1)}}\right)$ represent the sample size of set $U_{\alpha_{\mathrm{EL}(2)},\alpha_{\mathrm{EL}(1)}}$. As described in (22) and Fig. 3, the algorithm for s_1 is divided into three parts by the sample size N_0 of set $U_{\alpha_{\mathrm{EL}(2)},\alpha_{\mathrm{EL}(1)}}$. After the analysis of the requirement, the value of N_0 is set as 8.

There are three intermediate variables to obtain the final parameter s. The parameter s_{limit} is used to limit or bound the noise of pseudorange residuals relative to many error sources and can be computed by the standard deviation of the pseudorange residuals (or UEREs) (Blanch et al., 2012; Chen et al., 2017b, 2018). The variable s is used to evaluate pseudoranges (or UEREs) in real time, and further monitor the state of a specific satellite. UEREs are processed by CNMP algorithm and right tail CDF, and then used to deduce the variable s. The variable s_{DOP} takes the geometry between the satellite and monitor stations as another information source to compensate for the insufficient monitoring capability of monitor stations when the satellite is moving over the boundary of the monitoring network. The geometry information can be translated into s_{DOP} according to the relationship between them (Chen et al., 2017b; Shao et al., 2009, 2011b).

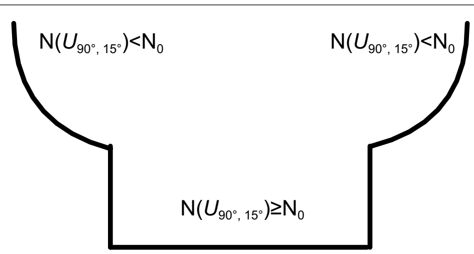

Fig. 3 Groove model for the parameter *s*

Finally, the covariance matrix for clock-ephemeris after the above processes is updated by

$$\boldsymbol{P}_3 = \frac{s_1^2}{P_{\max}} \left(\frac{K_{\mathrm{HMI}} + K_{\mathrm{bias}} + K_{\mathrm{pfa}}}{K_7}\right)^2 \boldsymbol{P}_{\mathrm{SCE}} \tag{23}$$

The matrix is used as the final covariance for clock-ephemeris errors which will be formatted into UDRE and MT28.

To broadcast the clock-ephemeris covariance, one needs to compress the matrix $\boldsymbol{P}_3$ into UDRE and MT28. Firstly, $\boldsymbol{P}_3$ is projected along the vector from the monitor station to a satellite, and the maximum of the projection is obtained by searching the service volume (Shao et al., 2011a; Zhao et al., 2014). Secondly, UDRE can be obtained by searching the lookup table of UDREI to bound the projection (SC-159, 2016). Thirdly, the matrix $\boldsymbol{C}$ to be broadcast can be determined by finding the optimal solution with the minimum of quantization error for the clock-ephemeris covariance (Chen et al., 2018; Kailath et al., 2000). Finally, UDRE and MT28 are determined and updated within their update interval.

Analysis and results

In this section, the performance of the proposed method (noted as ICB method) is compared with the direct statistic method (Li, 2018) and the latest WAAS covariance-based method noted as CB method which is not openly available, but updated from the old version (Walter et al., 2001; Wu & Peck, 2002). The direct statistic method stands for the latest method adopted in Chinese engineering practice. The covariance-based method refers to the method adopted by WAAS which shows the best performance and is considered as the latest covariance-based method. Therefore, the two methods are used as comparison. The analysis is presented to demonstrate the rationality and effectiveness of ICB method. As for data source, the broadcast ephemeris and observation data are from the websites of international GNSS service and national geodetic survey. The data is processed in monitor stations and master stations with the three methods to generate the corresponding satellite integrity information. The monitor stations located in North America shown in Fig. 4 are used to analyze the performance of ICB method. There are two parts in this section: the performance in the range domain and performance in the position domain (Chen et al., 2021). In the first subsection, the integrity bounding percentages between UDRE (along with MT28) and UERE are computed. In the second subsection, the availability is analyzed.

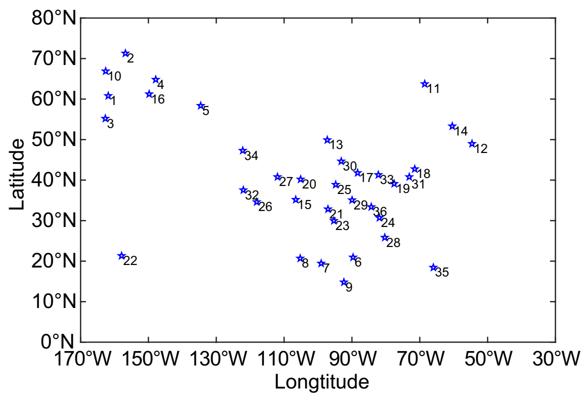

Fig. 4 Distribution of selected monitor stations

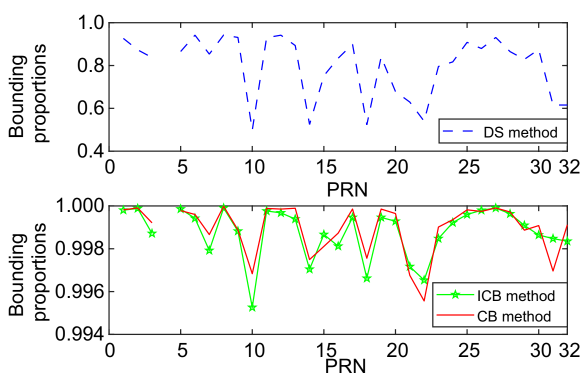

Fig. 5 Integrity bounding proportions of three methods

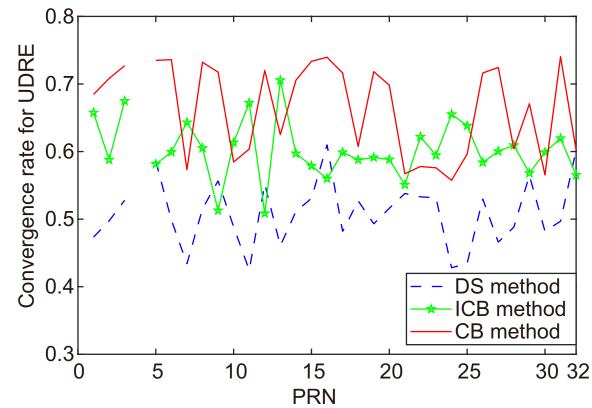

Fig. 6 UDRE convergence rate for each satellite

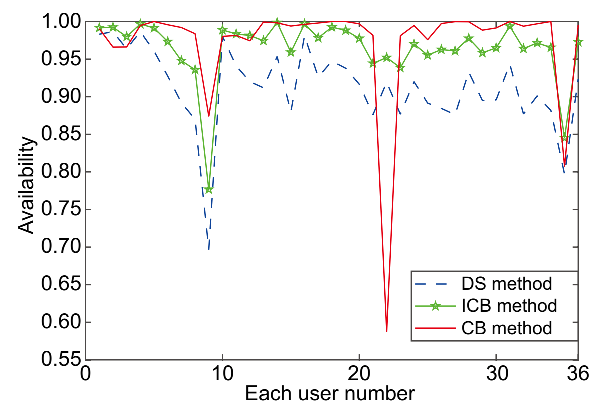

Fig. 7 Availability of LPV200 service at each selected user

Performance in the range domain

The integrity bounding percentages between UDRE (along with MT28) and UERE by ICB method are compared with these by the state-of-the-art methods (DS method and CB method).

The UDREs (along with MT28) of all GPS satellites are used to calculate the integrity bounding proportions with respect to 36 users (William, 2022). The mean of the integrity bounding proportions with the three methods for each satellite is depicted in Fig. 5. The mean of the integrity bounding proportions of DS method, ICB method, and CB method is 79.96%, 99.88%, and 99.90%, respectively. The integrity bounding rate of ICB method is 24.91% higher than that with DS method, close to the one with CB method. The integrity bounding proportion of ICB method is higher than that with DS method obviously.

Finally, the UDRE convergence rate for each satellite is calculated and shown in Fig. 6. As can be seen in Fig. 6, the convergence rate for the UDRE with ICB method is in between these with CB method and DS method. In detail, this indicator with ICB method is 8.04% higher than that with CB method and 19.90% lower than that with DS method. In other words, ICB method reveals a better performance in the aspect of safety. Short convergence time is significant for SBAS integrity monitoring, especially for BDSBAS, the GPS Aided GEO Augmented Navigation system (GAGAN), and the Mtsat Satellite-based Augmentation System (MSAS) whose monitor stations have smaller spacing compared with WAAS.

Performance in the position domain

The performance in the position domain is compared among the three methods in this subsection. The availability of LPV200 service is compared among three methods.

The availability of 36 users is analyzed as shown in Fig. 7. The mean of the availability of DS method, ICB method and CB method is 91.26%, 96.40%, and 97.15%, respectively. The availability by ICB method is 5.63%

higher than that by DS method and 0.77% lower than that by CB method. Considering that the users 9 and 22 are located in the boundary area of North America and their observations are very poor, the results are accidental and abnormal. The conclusion is the availability with ICB method is higher than that with DS method obviously and similar to that with CB method.

In a word, ICB method improved the integrity bounding rate and the availability dramatically compared with DS method. The performance of ICB method is close to that of CB method.

The signal-in-space errors of the proposed method and broadcast ephemeris method are smaller than that of WAAS method. The accuracy of signal-in-space of the proposed method is over 18.22% higher than that with broadcast ephemeris method in the three orbital dimensions while the accuracy of signal-in-space of WAAS method is lower than that of the broadcast ephemeris method in these three dimensions. The accuracy of signal-in-space of the proposed method is over 32.03% higher than that of WAAS method in orbit. As for satellite clock, the accuracy of signal-in-space of both the proposed method and WAAS method is lower than that of broadcast ephemeris method. The accuracy of signal-in-space of the proposed method is over 25.74% higher than that of WAAS method in clock. In total, compared with WAAS method, the proposed method can improve the accuracy of signal-in-space by over 25.74%. We can conclude that WAAS is designed to ensure the integrity at the expense of accuracy of signal-in-space and the proposed method can be used for some precise positioning application (Zheng et al., 2019, 2022).

The influence of different parameter values involved in the Groove Model has been analyzed. A detailed analysis of integrity needs too many observations because it is relative to many monitor stations and its layout. For simplicity, the experiences tell that the more conservative the parameter N_0, the higher the integrity in the edge area of the monitoring network will be and the lower service availability.

Also, the proposed method is applied for satellite integrity monitoring in China. The results reveal that compared with the direct statistic method, the integrity bounding rate in the pseudorange domain and the availability in the position domain are improved by 45.39% and 2.32%, respectively. The proposed method can provide APV-I services for the most parts of China and even LPV200 services for some parts of China (Zheng et al., 2022). The proposed method was tested with just a set of Chinese receivers at a monitor station, and the performance is satisfactory with limited quality monitor stations and their limited layout, which can be used for satellite integrity monitoring in south China of the inverted triangle and the edge area of the monitoring network.

Discussions and conclusions

An improved covariance-based method is developed to perform satellite integrity monitoring. Compared with the direct statistic method, the integrity bounding percentage is improved by 24.91% and the availability by 5.63%. Compared with the covariance-based method, the convergence rate for user differential range errors is improved by 8.04%. The advantages of the proposed method are summarized as follows:

1. The proposed method concerns both the integrity and the availability. The clock-ephemeris covariance matrix is adjusted by considering threat models and Gaussian overbounding theory to guarantee that the parameter UDRE along with MT28 bounds the range error from clock-ephemeris with a high probability.
2. The scale model and groove model are beneficial for understanding the concept of SBAS integrity. These models are used to address the problem of the inaccurate estimation of clock-ephemeris covariance considering the geometry between satellites and monitor stations. The scale model is used to adjust the covariance matrix of clock-ephemeris with the consideration of abnormal cases. The groove model considers the geometry between satellites and monitor stations, which is used as prior information to compensate for the insufficient monitoring capacity of monitor stations when a specific satellite is moving over the boundary of the monitoring network. The groove model mitigates random errors or integrity threats, improves the accuracy of satellite integrity information, and provides an idea to perform satellite integrity monitoring by considering the motion process of a monitored satellite above its monitoring network, which is beneficial for improving the tracking capability of the monitoring network with respect to the satellites just over its boundary.

In a word, the proposed method can provide LPV200 service for most North America. To improve the performance further, it is still necessary to investigate some other issues in the future. One important issue is that the data preprocessing of monitor stations needs to be optimized due to its impact of data quality and even satellite integrity monitoring, which is the key to improve the integrity bounding rate. Another issue is related to the reliability of the proposed method. The availability at some selected users is not adequate and the method needs to be refined to guarantee its robustness. Future work will include the optimization of the preprocessing of monitor stations and the improvement of the reliability of the proposed method.

Acknowledgements
Not applicable.

Author contributions
Conceptualization: SZ, ZH and XJ; Methodology: SZ; Writing original draft: SZ; Editing: XJ and MG; Review: MG, XJ and KL. All authors read and approved the final manuscript.

Funding
This research is supported by the Research Startup Funds from Tianjin University of Technology under Grant 01002101.

Availability of data and materials
Not applicable.

Declarations

Competing interests
The authors declare that they have no competing interests.

Author details
[1]School of Integrated Circuit Science and Engineering, Tianjin University of Technology, No. 391 Bin Shui Xi Dao Road, Xiqing District, Tianjin 300384, China. [2]School of Electronic and Information Engineering, Beihang University, No. 37 Xueyuan Road, Haidian District, Beijing 100191, China. [3]Tianjin Navigation Instrument Research Institute, No. 268 No. 1 Road, Ding Zi Gu Street, Hongqiao District, Tianjin 300131, China.

Received: 7 December 2021 Accepted: 18 April 2022
Published online: 09 May 2022

References

Blanch, J., Walter, T., & Enge P. (2012). A clock and ephemeris algorithm for dual-frequency SBAS. In *Proceedings of the ION GNSS 2012*, Portland, OR (pp. 2513–2519).
Blanch, J., Walter, T., Enge, P., Stem, A., & Altshuler, E. (2014). Evaluation of a covariance-based clock and ephemeris error bounding algorithm for SBAS. In *Proceedings of the ION GNSS 2014*, Florida, USA (pp. 3270–3276).
Chen, J., Huang, Z. G., Li, R., & Gao, W. G. (2017a). An efficient algorithm for determining the correspondence between DFREI and s DFRE for a dual-frequency multi-constellation satellite-based augmentation system. In *the 10th China Satellite Navigation Conference 2017a*, Shanghai, China, (pp. 109–118).
Chen, J., Wang, J., & Yuan, H. (2021). Performance analysis of a GNSS multipath detection and mitigation method with two low-cost antennas in RTK positioning. *IEEE Sensors Journal*, *22*(6), 4827–4835.
Chen, J. P. (2001). *Research of GPS integrity augmentation* (pp. 10–110). Information Engineering University.
Chen, J., Huang, Z. G., & Li, R. (2017b). Computation of satellite clock-ephemeris corrections using a priori knowledge for satellite-based augmentation system. *GPS Solutions, 21*(2), 663–673.
Chen, J., Huang, Z. G., & Li, R. (2018). Computation of satellite clock-ephemeris augmentation parameters for dual-frequency multi-constellation satellite-based augmentation system. *Journal of Systems Engineering and Electronics, 29*(6), 1111–1123.
Decleene, B. (2000). Defining pseudorange integrity – overbounding. In *Proceedings of the ION GPS 2000*, Salt Lake City, UT, USA (pp. 1916–1924).
Hamada, M. (2008). *Bayesian reliability* (pp. 85–317). Berlin, Germany: Springer Science & Business Media.
Hwang, P., McGraw, G., & Bader, J. (1999). Enhanced differential GPS carrier-smoothed code processing using dual-frequency measurements. *Navigation-US, 46*(2), 127–137.
Kailath, T., Sayed, A., & Hassibi, B. (2000). *Linear estimation* (pp. 103–132). Prentice Hall.
Konno, H., Pullen, S., Rife, J., & Enge P. (2006). Evaluation of two types of dual-frequency differential GPS techniques under anomalous ionosphere conditions. In *Proceedings of the ION NTM 2000*, Monterey, CA, USA (pp. 735–747).
Li R. (2018). *Studies on the wide-area differential correction for BeiDou global satellite navigation system* (pp. 1–100). University of Chinese Academy of Sciences.
Li, R., Cao, Y., Hu, X., Tang, C., Zhou, S., Meng, X., Liu, L., Su, R., & Chang, Z. (2018). Analysis of the wide area differential correction for BeiDou global satellite navigation system. *Research in Astronomy and Astrophysics, 18*(11), 19–30.
Li, R., Hu, X., Cao, Y., Tan, C., Meng, X., & Chang, Z. (2019). Research on ephemeris and clock corrections algorithm for BeiDou wide area differential augmentation system. *Process in Astronomy, 37*(1), 80–110.
Li, R., Zheng, S. Y., Wang, E. S., Chen, J. P., Feng, S. J., Wang, D., & Dai, L. W. (2020). Advances in BeiDou navigation satellite system (BDS) and satellite navigation augmentation technologies. *Satellite Navigation, 1*(1), 1–23.
Lu, X., Chen, L., & Shen, N. (2021). Decoding PPP corrections from BDS B2b signals using a software-defined receiver: An initial performance evaluation. *IEEE Sensors Journal, 21*(6), 7871–7883.
Meng, Q., & Hsu, T. L. (2021). Integrity monitoring for all-source navigation enhanced by Kalman filter-based solution separation. *IEEE Sensors Journal, 21*(14), 15469–15484.
Parkinson, B., Enge, P., Axelrad, P., & Spilker, J. (1996). *Global positioning system: theory and applications* (Vol. ii, pp. 81–150), Virginia: American Institute of Aeronautics and Astronautics.
SC-159. (2016). Minimum operational performance standards for global positioning system/satellite-based augmentation system airborne equipment. RTCA DO-229 (pp. 1–500).
SC-167. (1992). Software considerations in airborne systems and equipment certification. RTCA DO-178B (pp. 1–120).
Schempp, T., Peck, S., & Fries, R. (2001). WAAS algorithm contribution to hazardously misleading information (HMI). In *Proceedings of the ION GPS 2001*, Salt Lake City (pp. 1831–1837).
Shallberg, K., Shloss, P., Altshuler, E., & Tahmazyan, L. (2001). WAAS measurement processing reducing the effects of multipath. In *Proceedings of the ION GPS 2001*, Salt Lake City (2334–2340).
Shallberg, K., & Sheng, F. (2008). WAAS measurement processing: current design and potential improvements. *IEEE/ION position location and navigation symposium 2008*, Monterey, CA, USA (pp. 253–262).
Shao, B., Liu, J., Huang, Z. G., & Li, R. (2009). A PSO based algorithm for optimizing distribution of reference stations in SBAS. *International conference on information engineering & computer science*, no. 1 (pp. 110–113).
Shao, B. (2012). *Research on integrity key technology of user differential range error for mixed constellation* (pp. 1–130). Beihang University.
Shao, B., Liu, J., Huang, Z. G., & Li, R. (2011b). A parallel particle swarm optimization algorithm for reference stations distribution. *Journal of Software, 6*(7), 1281–1288.
Shao, B., Liu, J., Zhao, R. B., Huang, Z. G., & Li, R. (2011a). A user differential range error calculating algorithm based on analytic method. *Chinese Journal of Aeronautics, 24*(6), 762–767.
Tsai, Y. (1999). *Wide area differential operation of the global positioning system: ephemeris and clock algorithms* (pp. 1–101). California: Department of Mechanical Engineering, Stanford University.
Walter, T., Hansen, A., & Enge, P. (2001). Message type 28. In *Proceedings of the ION GNSS 2001*, Long Beach (pp. 522–532).
William, J. (2022). Wide area augmentation system performance analysis report#79. FAA.
Wu, J., & Peck, S. (2002). An analysis of satellite integrity monitoring improvement for WAAS. In *Proceedings of the ION GPS 2002*, Portland, OR, September 24–27 (pp. 756–765).
Yin, X., & Chai, H. (2020). Constrained robust unscented Kalman filter for BDS navigation in dense urban areas. *IEEE Sensors Journal, 21*(3), 3077–3086.

Zhao, R. B., Li, R., Huang, Z. G., & Shao, B. (2014). A user range accuracy estimation method of the global navigation satellite system. *Chinese Journal of Electronics, 23*(1), 194–198.
Zheng, S. Y., Gao, M. Z., Li, K., Jin, X. Q., Qin, J., Xia, D. (2022). Potential performance of satellite-based augmentation system based on CMONOC in China. In *The 13th China Satellite Navigation Conference 2022*, Beijing, China, Accepted 2022.
Zheng, S. Y., Li, R., Huang, Z. G., & Shao, B. (2019). Determination of fast corrections for satellite-based augmentation system. *IEEE ACCESS, 7*, 178662–178674.

Publisher's Note